Synthesis and Characterization of Novel Schiff Base Polymers as Adsorbents for the Removal of Mercuric Ion from Aqueous Solution

R. Santhi[1,*,] and B. Rajeswari[1,2,]

[1]P.G. and Research Department of Chemistry, Seethalakshmi Ramaswami College (Affiliated to Bharathidasan University), Tiruchirappalli-620002, India
[2]Department of Chemistry, K. Ramakrishnan College of Engineering, Samayapuram, Tiruchirappalli-621112, India

*Corresponding author: E-mail: santhichemsrc@gmail.com

The primary objective of this study is to synthesize polymeric adsorbents and assess the analytical effectiveness of novel organic composites using the batch mode of adsorption. Hence, the organic polymers were prepared by doping the Schiff bases on polyaniline chloride by chemical oxidation method. The prepared polymeric composites were characterized using UV-visible, FT-IR and ^{1}H NMR spectral techniques. An attempt was made to investigate adsorption capacity of synthesized polymers for the removal of mercuric ion by varying the various factors such as initial concentration of adsorbates, temperature, contact time, pH, concentration of adsorbents. Sorption isotherms were constructed using Langmuir, Freundlich, Dubinin Radush Kevich, Temkin and Redlich Peterson models. The SEM micrograph and PXRD spectra were also recorded to confirm the metal ion adsorption on the surface of investigated composites.

Keywords: Adsorption, Polymeric composite, Mercuric chloride, Tryptamine, Tryptophan, Schiff bases.

INTRODUCTION

Now a day's effluents from the chemical industries are found to be contaminated with heavy metals. These heavy metals are toxic to living system and it becomes mandatory to either eliminate or to minimize the amount of their level of adsorption by animals and human beings [1-6]. Adsorption, ion exchange, membrane filtration, flocculation, coagulation and chemical precipitation are the various methods available for the removal of heavy metal ions from the aqueous medium [7,8].

According to world health organization (WHO), mercury is one of the most harmful substances for human health [9]. It can influence the nervous system, brain development and much more [10-13]. Further, mercury spreads very easily through nature and food chain [14,15]. In recent years, reducing the harmful level of mercury from large amount of water by an efficient method is a challenging task. The adsorption technique is reported to be the most suitable method for the treatment of contaminated wastewater by removing various types of pollutants and thus attract the researchers to meet out the global need [16-21]. This technique is the most suitable method due to its effectiveness even at low concentrations, selectivity, regen-

eration of used adsorbents and cost efficiency. The primary objective of this study is to synthesize novel organic polymers containing Schiff bases and utilize these newly developed adsorbents for the batch mode removal of heavy metal ions.

EXPERIMENTAL

The solvents and reagents of AR grade were used. Distilled aniline was used in all the cases whereas double distilled water was used to prepare all the solutions. In order to understand the sorption behaviour of the adsorbate at various pH, BDH samples of HCl and NaOH were used.

Synthesis of Schiff base: The Schiff base was synthesized from terephthalaldehyde and tryptamine (1:2) and mixed at room temperature by grinding both compounds in the presence of acetic acid [22]. The mixture was then refluxed for 6 h and the solid products obtained was filtered using the suction pump. The crude product was washed thoroughly from ethanol and finally dried over anhydrous calcium chloride (**Scheme-I**).

The Schiff bases N-(2-chlorobenzylidene)-2-(1*H*-indol-3-yl)ethanamine (T2ClB), (*E*)-2-((2-chlorobenzylidene)amino)-3-(3a,7a-dihydro-1*H*-indol-3-yl)propanoic acid (TP2ClB),

Scheme-I: Preparation of Schiff base
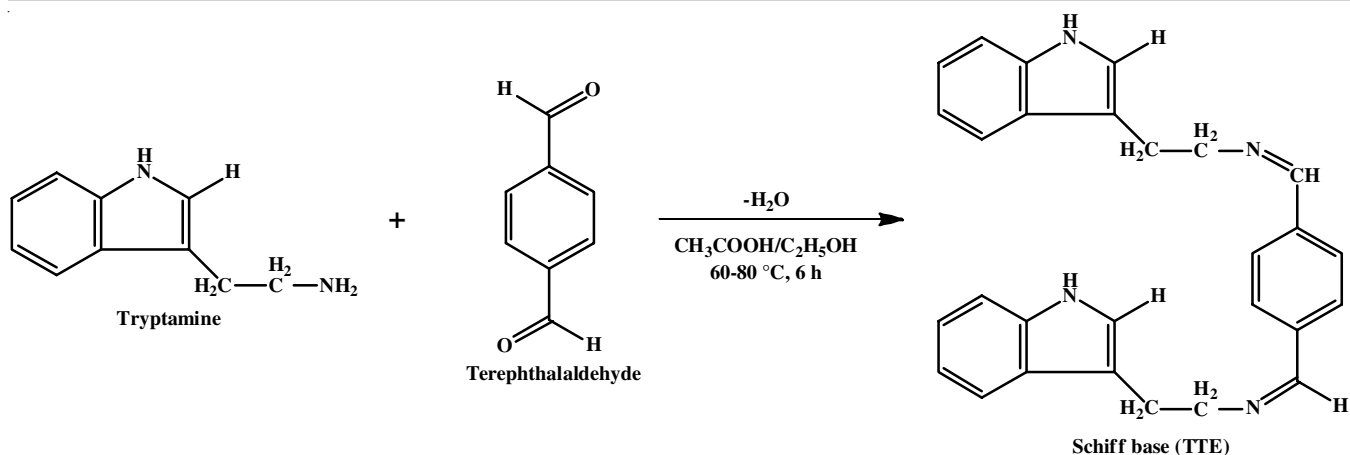
N,N′-(1,4-phenylenebis(methanylylidene))*bis*(2-(1*H*-indol-3-yl)ethanamine) (TTE), 2,2′-((1Z,1′E)-(1,4-phenylenebis-(methanylylidene))*bis*(azanylylidene))*bis*(3-(3a,7a-dihydro-1*H*-indol-3-yl)propanoic acid) (TPTE) were synthesized and characterized using standard procedure [23].

Synthesis of polyaniline chloride: A 50 mL of potassium persulphate (0.1 M) was added dropwise to aniline (0.1 M) dissolved in 1 M HCl with continuous stirring using a magnetic stirrer for about 2 h at 303 K. The contents were stirred further for 30 min to ensure complete polymerization. A dark green coloured PANICl was filtered using a Whatmann No. 1 filter paper. The excess acid content and oligomers of aniline were removed by repeated washings with distilled water, ethanol, acetone and diethyl ether. The green coloured polymer obtained was dried in an air oven for 4 h till constant weight was reached.

The colour changes that appeared during the addition of potassium persulphate is shown as below:

Straw yellow → yellow → brown → green colour

Preparation of polymeric composite: Mixture of PANICl (1 g) and Schiff base (1 g) were suspended in 25mL of diethyl ether and allowed to sonicate in an ultrasonic cleaning bath (NEY, 50 Khz) for 0.5 h. The resulting slurry was centrifuged and then centrifugate was removed. The final produt was washed with diethyl ether and again centrifuged. A dark green coloured compound was dried in a vacuum desiccators (**Scheme-II**).

Characterization: Electronic spectra of the prepared composites were recorded using Lambda 35 Perkin Elmer UV-visible spectrophotometer (200-1100 nm) with DMSO as solvent. Perkin-Elmer FTIR spectrometer was used to record FTIR spectra. Proton NMR spectra was studied in DMSO using Bruker 400 MHz Nuclear Magnetic Resonance spectrometer. After adsorption of mercuric ion, the Powder XRD of the adsorbent was recorded using Bruker D8 X-ray diffractometer, Germany at a scan rate of 1 step/s. The surface morphology of the samples was observed using a field emission scanning electron microscope (JSM 6700F model; JEOL, Japan).

Sorption studies: The polyaniline composites (2 mg) were mixed with mercuric chloride solution (10 mL, 0.02 M) and subjected to sonication for 30 min at room temperature and centrifuged. The conductometric titration methods [24] were used to determine the concentration of mercuric ion in the supernatant liquid. The initial concentrations (C_o) were in the range of 0.01-0.05 M.

Effect of temperature: In the temperature range of 303-318 K, the adsorption characteristics of PANI-Schiff base composites were studied to understand the effect of temperature following the same batch process.

Effect of contact time: An adsorbent of 2 mg was sonicated with 0.02 M HgCl$_2$ solution and 30 min was found to be a suitable time period in order to understand the effect of sonication time.
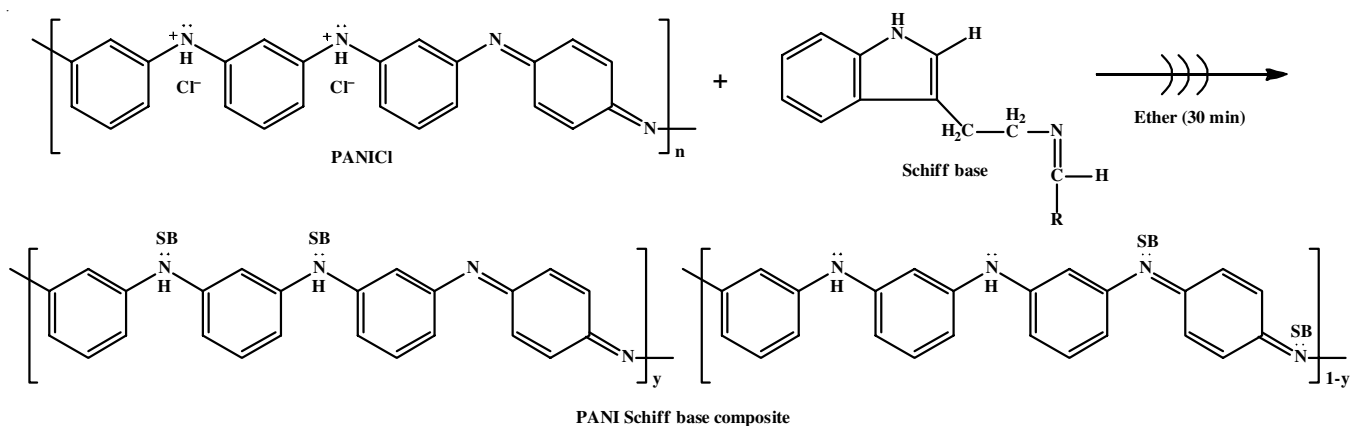

Scheme-II: Preparation of polymeric composites (SB = Schiff base)

TABLE-1 PHYSICAL DATA OF THE COMPOUNDS						
Schiff base	Colour	m.p. (ºC)	Yield (%)	Elemental analysis (%): Calcd. (exp.)		
				C	H	N
T2ClB	Pale yellow	214	70	63.90 (63.90)	6.06 (6.05)	8.67 (8.69)
TTE	Sandle	185	75	78.26 (78.10)	6.20 (6.00)	15.40 (15.20)
TP2ClB	Sandle	173	70	65.80 (65.60)	5.20 (5.00)	8.50 (8.30)
TPTE	Light white	130	65	71.10 (70.80)	5.10 (4.90)	11.10 (10.90)

Effect of pH: The effect pH on the adsorption efficacy of PANI-Schiff base composites were studied in the pH range 1-13. To maintain the low pH, HCl was used and for more than pH 7, sodium hydroxide was used.

RESULTS AND DISCUSSION

The Schiff bases and polymeric composites were synthesized by general methods. The yield was good and all compounds were found to be stable. The physical properties of the synthesized compounds are mentioned in Table-1.

Spectral characterization of Schiff bases

Electronic spectra: Electronic spectra of all the Schiff bases were recorded in DMSO solvent in the range of 200-700 nm at room temperature. Compound *N,N′*-(1,4-phenylene-bis(methanylylidene))*bis*(2-(1*H*-indol-3-yl)ethanamine) (TTE) exhibit two bands due to π-π* and n-π* transitions. The intense bands at 302 nm may be assigned to π-π* transition of the aromatic groups present in a compound. The absorption bands at 341 nm may be due to the n-π* transitions of the imine group present in Schiff bases.

FTIR spectra: The FT-IR spectra of the prepared compounds exhibit imine peaks in the range 1641-1589 cm^{-1}. Absence of characteristic peaks due to the carbonyl group of aldehydes and ketones at 1700 cm^{-1} and the appearance of azomethine bands confirms the formation of Schiff bases. The absorption bands at 3400-3223 cm^{-1} ascribed to N-H stretching vibrations of indole group. The bands in the range of 1442 cm^{-1}-1535 cm^{-1} may be due to ν(C=C) stretching vibrations of aromatic rings. The bands appear in the region of 3038-2355 cm^{-1} corresponds to the aromatic and aliphatic O-H groups. The broad peaks in the region 1100-1000 cm^{-1} may be attributed to C-N stretching vibrations of primary amines. The peaks observed in the region 1476-1408 cm^{-1} can be assigned to C-C stretching vibrations of aromatic ring. The bending vibrations of various groups are found in the region 960-400 cm^{-1}. The bending vibrations below 600 cm^{-1} may be attributed to OH and Cl substituents present in carbonyl compounds [25].

^{1}H NMR spectra: A singlet observed at δ 7.9-8.3 ppm for the compound TTE confirms the formation of Schiff bases. A sharp singlet at δ 10.8-11 ppm indicates the presence of NH proton of indole group. The multiplets observed in the region of δ 6.9-7.5 ppm for all the compounds are due to the presence of aromatic protons in tryptamine and carbonyl compounds. The two aliphatic –CH$_2$ protons of tryptamine group are found at δ 2.5- 3.1 ppm.

Characterization of polymeric composites

UV-visible spectra: The UV-visible absorption spectra of the PANI-Schiff base composites generally depend on the nature of dopants, extent of conjugation and solvent employed for recording the spectrum. All the investigated polymers exhibit two bands around 256-382 nm due to the π-π* transitions in the aromatic rings [25] (Table-2). A change in the percentage composition of the benzenoid and quinanoid forms after mercuric ion adsor-ption is represented by the shift in λ$_{max}$ values. Compound (*E*)-2-((2-chlorobenzylidene)amino)-3-(3a,7a-dihydro-1*H*-indol-3-yl)-propanoic acid (TP2ClB) shows a minimum shift in λ$_{max}$ values after the adsorption of metal ion. A bathochromic shift observed in polymers PTP2ClB, PTPTE confirmed the adsorption of mercuric ion. The adsorption of metal ion on the compound PTTE is evidenced by a small shift in λ$_{max}$ values towards the lower wavelength.

TABLE-2 UV-VISIBLE SPECTRA OF PANI SCHIFF BASE COMPOSITES		
Polymer	λ$_{max}$ (nm)	
	π–π*	n–π*
PANICl	310	583
PANICl-HgCl$_2$	260	585
PT2ClB	258	281
PT2ClB-HgCl$_2$	258	283
PTTE	285	698
PTTE-HgCl$_2$	268	289
PTP2CLB	265	–
PTP2CLB-HgCl$_2$	268	279, 289
PTPTE	217	263
PTPTE-HgCl$_2$	268, 279	289

FTIR spectra: FTIR spectral studies of PANI-Schiff base composites provide information about the presence of amino and imine groups in polymer chain, benzenoid/quinonoid forms, polymer back bone and structural changes due to the doping of Schiff bases on PANI matrix (Table-3).

The presence of absorption bands in the range 4000-3500 cm^{-1} may be ascribed to -OH stretching frequency of -COOH group of tryptophan molecule in Schiff base doped on PANI chloride. The presence of sharp bands in the range of 1683-1617 cm^{-1} indicate the CH=N moiety of Schiff bases. The presence of iminobenzenoid rings in PANI backbones are estabilished by the appearance of signature peaks around 1514-1487 cm^{-1}. The -OH bending mode of vibrations were observed at 990-940 cm^{-1} and the broad peaks at 1100-1000 cm^{-1} may be due to C-N stretching vibrations of primary amine moiety. Peaks at 690-600 cm^{-1} may be due to the bending vibrations of PANI matrix. The doping of Schiff base on the composite is further evidenced by the presence of the peak at 597 cm^{-1} ν(C-Cl).

^{1}H NMR spectra: The ^{1}H NMR spectra of the polymeric composites exhibit signal at δ 10-11 ppm may be attributed to

TABLE-3
FTIR SPECTRA (cm^{-1}) OF PANI SCHIFF BASE COMPOSITES

Polymer	ν(OH)	ν(NH)	ν(C-H)	ν(C=N)	ν(C=C)	ν(C-NH), ν(C-C), ν(C-O)	δ(C-C), δ(C-H), δ(C-N), δ(C-OH)	Δ(I), δ(Cl), δ(OH)
PT2ClB	3470	3259, 3055	2924, 2854, 2610, 2511	2099, 1617	1491, 1436	1391, 1318, 1266, 1215, 1184, 1110, 1104, 1154, 1016	999, 875, 807, 744, 650, 616	515, 491, 474, 460
PT2ClB-HgCl$_2$	3407	–	2927, 2856	2100, 1607	1494	1391, 1302, 1122, 1000	873, 807, 746, 692, 648	494, 406
PTTE	3500	3259, 3055, 2924, 2959	2854, 2610, 2511, 2099	1617, 1577	1491, 1436, 1391, 1318, 1266	1215, 1184, 1154, 1110, 1047, 1016	899, 875, 807, 744, 650, 616	517, 474, 491, 410
PTTE- HgCl$_2$	3853, 3785	3353, 2962, 2925, 2794, 2605, 2493	1934	1692, 1609	1451, 1336, 1300, 1271	1212, 1110, 1045, 1009, 900	828, 799, 740, 620	579, 544, 507, 486, 430, 407
PTP2ClB	3853, 3781	3428, 2926	–	1624	1468, 1387	1270, 1118, 1045	869, 749, 644	531, 469
PTP2ClB-HgCl$_2$	3911	3336, 2922	–	1702, 1619	1427, 1468, 1402, 1381	1338, 1269, 1231, 1204, 1116, 1110, 1069	816, 765	615
PTPTE	–	3391, 3056	2946, 2793, 2500	1626	1450, 1432, 1388	1306, 1269, 1223, 1145, 1113, 1090, 1043, 1013	967, 839, 743	594, 509, 430
PTPTE - HgCl$_2$	3697, 3625	3383	–	1793, 1701, 1531	1367	1308, 1219, 1036	710, 609	546
PANICl	3934, 3820, 3713	3423	2985, 2573, 2358, 2078	1692, 1588	1487	1293, 1239, 1124	798	505

–OH proton of carboxylic acid group of the dopant molecule. The signal at δ 8.2 ppm confirms the presence of imine protons of Schiff bases. The signals around δ 7.1-7.6 ppm can be attributed to aromatic –NH and –CH protons. The peaks at δ 6.7-6.9 ppm may be due to the CH protons of quinoid rings (Table-4).

XRD studies: Several sharp peaks in the region of 10-70º (2θ) with a step size of 0.001º were observed in powder XRD spectrum. The average particle size (D) was calculated from Debye-Scherrer's formula (eqn. 10).

$$D = \frac{0.9\lambda}{\beta\cos\theta} \qquad (10)$$

where λ = wavelength of CuK_α radiation (1.54 Å), β = full width at half maximum of peaks. The generated PANI composites show the nano structure of polymers with particle sizes ranging from 23 to 85 nm. The crystalline character of polymeric composites is demonstrated by the strong peaks in the area of 20-63º (Table-5). The presence of prominent peaks further supports the hypothesis that metal ions are being adsorbed onto the PANI matrix. The PANI skeleton may be the cause of the peaks with 2θ values in the range of 20-21º for all the composites.

SEM studies: Adsorption of HgCl$_2$ on the PANI matrix is supported by the variation in morphology shown in the SEM micrographs of the polymeric composites taken before and after the process (Fig. 1a-h). Prior to adsorption, the particles are small, spherical in nature, but after adsorption, the particles are bigger, rod-shaped and their size distribution is not uniform. The embedded HgCl$_2$ molecules are clearly visible on the PANI backbone molecule.

TABLE-4
^{1}H NMR SPECTRA (ppm) OF PANI SCHIFF BASE COMPOSITES

| Polymeric composite	N-H	CH=N	Benzenoid protons C-H indole proton	Quinoid protons phenyl C-H	Aliphatic C-H
PT2ClB	10.652(s) 9.3 (s)	8.636 (s)	7.89-7.75 (d), 7.731-7.37(m), 7.18-6.97(m),	6.063-5.96(d), 5.87 (s), 5.80-5.68 (s)	3.130-3.07 (s), 2.87-2.739 (m), 2.508 (s)
PTTE	10.74-10.69 (d), 10.048 (s)	7.97-7.94 (d)	7.58-7.482 (dd), 7.39-7.38 (d), 7.297-7.25 (t)	7.103-6.98 (m), 5.631-5.92 (d)	3.39 (s), 3.24-3.21(t), 2.925-2.903 (d), 2.507 (s)
PTP2ClB	-	-	7.796-7.771(d), 7.552-7.510 (s), 7.459-7.435(s)	-	3.63 (s), 2.508 (s)
PTPTE	10.77-10.74 (d), 10.72-10.45 (t), 10.05-10.01 (d)	7.96-7.88 (dd)	7.67-7.62 (d), 7.53-7.488 (d), 7.454-7.35 (dd), 7.32-7.27(d), 7.24-7.216(d)	7.15-6.958 (m)	5.52-5.47 (d), 3.94-3.89 (d), 3.75-3.71(m), 3.18-3.13 (d), 2.94-2.86 (d), 2.508(s), 1.917 (s)
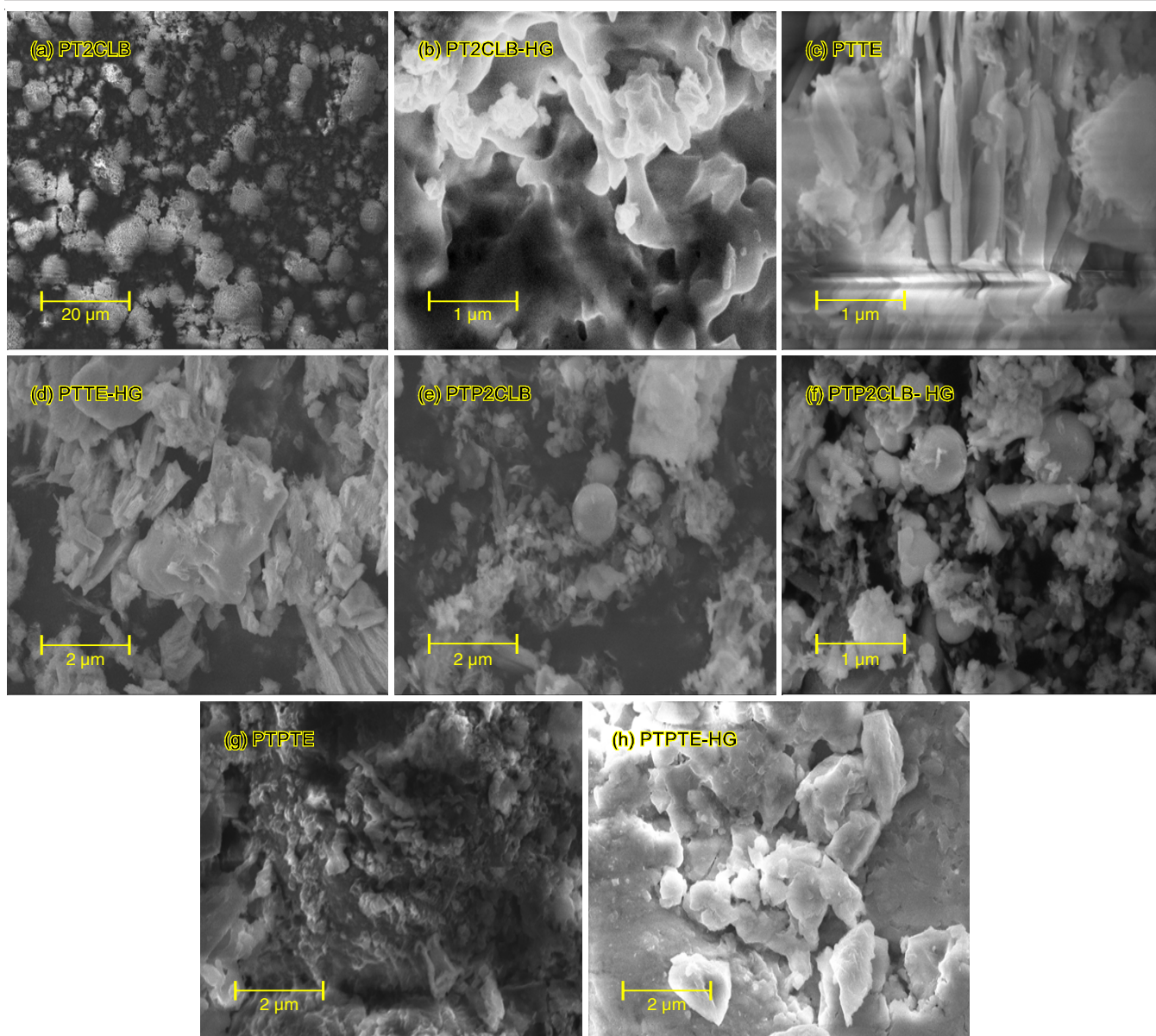
Fig. 1. SEM analysis of before and after adsorption of HgCl$_2$ on PANI-Schiff base composites

TABLE-5
XRD ANALYSIS OF POLYMERIC COMPOSITES

Polymer	2θ	Particle size (nm)
PT2CLB	21.6, 23.9, 27.5	27.2-80.8
PTTE	20.4, 21.5, 27.4	32.7-40.4
PTP2CLB	20.4, 25.5, 27.5, 33.3	55.4
PTPTE	20.460, 23.991, 26.378, 27.489, 20.46- 27.49	32.71-40.6

Sorption experiments

Effect of mercuric chloride: Adsorption of HgCl$_2$ on polymeric composites were studied through batch process. For all the adsorption processes, the reactant mixtures were equilibrated for 30 min. After the adsorption process is over, the concentration of mercuric ions was measured conductomerically using KI as standard solution. The change in the adsorbate concentrations after adsorption equilibrium determines the adsorption capacity of adsorbents. For all the polymeric composites the q$_e$ values increase with increase in concentration of mercuric ions.

Adsorption isotherms: The adsorption isotherms are helpful to explore the adsorbate–adsorbent interaction and determine the capacity of adsorbent when the adsorption process reaches an equilibrium state. The physical and chemical parameters obtained from the Langmuir, Freundlich, D-R, Temkin and Redlich-peterson isotherm models offer insight into the adsorption mechanisms, surface characteristics and efficacy of the adsorbent [26-28].

Langmuir model: To determine the amount of Hg^{2+} ions adsorbed (q$_m$) on the polymeric composites, this model is utilized. It is presumptively true that adsorption can only take place at a limited number of fixed, localized locations that are equal and equivalent, with no steric barrier between the molecules being adsorbed, even on nearby locations. When the adsor-

bate is stationary on the surface, it is used for homogeneous adsorption and reactions. It can be seen from the $1/q_e$ *vs.* $1/C_e$ figure that the process follows the Langmuir model. The slope and intercept of the plots are used to get the Langmuir constants q_m and K_L for each composite.

$$\frac{1}{q_e} = \frac{1}{K_L q_m C_e} + \frac{1}{q_m} \tag{1}$$

The maximal monolayer adsorption capacity of the adsorbent is represented by q_m in Langmuir equation (eqn. 1).

The separation factor, R_L, a dimensionless constant, can be used to describe the basic properties of Langmuir isotherm.

$$R_L = \frac{1}{1 + K_L C_o} \tag{2}$$

where K_L is Langmuir constant and C_o is initial concentration of adsorbate. The R_L values indicate that the adsorption process using the adsorbents under investigation is favourable ($0 < R_L < 1$) for all the PANI-Schiff base composites. Therefore, the Langmuir model is best fitted for all the PANI-Schiff base composites.

Freundlich isotherm: This model is based on the concept that adsorption takes place uniformly across all sites, with higher affinity sites being filled before lower affinity sites. Eqn. 3 represents the Freundlich adsorption isotherm, which provides the sorption equilibrium for both monolayer and multilayer adsorption.

$$\log q_e = \log k_F + \frac{1}{n} \log C_e \tag{3}$$

where k_F stands for adsorption capacity and n is a measure of adsorption intensity. The Freundlich isotherm constants, k_F (sorption capacity) and $1/n$ (sorption intensity) values are determined from the plot of $\log q_e$ *vs.* $\log C_e$. Table-6 displays

the correlation coefficients R^2. The fact that $n > 1$ indicates that adsorption is a favourable process.

Dubinin- Radushkevich (DR) isotherm: The linear form of DR isotherm is represented as:

$$\ln q_e = \ln qD - B\varepsilon^2 \tag{4}$$

The constants qD and B were determined from the slope and intercept are shown in Table-6 along with the linear slope of $\ln q_e$ *vs.* 2 plot. The Dubinin-Radushkevich (DR) isotherm is typically used to determine whether a metal ion is adsorbing by chemisorption or physisorption. According to this model, the physical nature of adsorption is better suited for all the composites under investigation ($B > 1$).

Temkin isotherm: This isotherm is utilized to comprehend the interactions between the adsorbent and adsorbate. Eqn. 5 is used to represent the linear form of Temkin isotherm:

$$q_e = B_T \ln A_T + B_T \ln C_e \tag{5}$$

The slope and intercept of the plot of q_e *vs.* $\ln C_e$ were used to compute the Temkin isotherm equilibrium binding constant (A_T) and the Temkin heat of adsorption (B_T). Temkin isotherm presupposes that, due to sorbate-sorbent interactions, the decline in heat of adsorption will be linear rather than logarithmic as indicated in the Freundlich equation and that the heat of sorption of all the molecules in the layer will decrease linearly with coverage. The binding constant A_T and Temkin heat of adsorption B_T are found to be high for PTTE (Table-6).

Redlich-Peterson isotherm: Redlich-Peterson isotherm can be applied for homogeneous or heterogeneous systems due to its versatility. The mathematical relation of this isotherm is given by eqn. 6:

$$\frac{C_e}{q_e} = \frac{1}{K_{RP}} + \frac{\alpha_{RP}}{K_{RP}} C_e \beta \tag{6}$$

TABLE-6
ISOTHERMAL PARAMETERS OF SORPTION ISOTHERMS FOR ALL THE ADSORBENTS

Isotherm	Parameters	PANI Cl	PT2ClB	PTTE	PTP2ClB	PTPTE
Langmuir	K_L	3.335	5.991	50	78.66	51.54
	q_m	16.94	17.4	6.02	23.5	3.37
	R^2	0.995	0.997	0.978	0.933	0.978
	R	0.997	0.998	0.988	0.965	0.988
	R_L	0.239	0.029	0.003	0.002	0.003
Freundlich	N	0.966	0.885	0.560	1.257	1.869
	K_F (L/mg)	2.978	2.197	29.78	43.65	27.79
	R^2	0.976	0.989	0.996	0.929	0.978
	R	0.987	0.994	0.997	0.964	0.988
Dubinin-Radushkevich	q_D (mg/g)	0.002	0.041	25.76	0.547	0.048
	B	1.535	0.188	4.344	1.167	1.045
	R^2	0.962	0.984	0.994	0.901	0.976
	R	0.981	0.992	0.997	0.949	0.987
Temkin	B_T (L/mg)	0.378	0.026	0.247	0.139	0.077
	A_T (KJ/mol)	1.024	1.001	1.140	1.039	1.0
	R^2	0.943	0.924	0.980	0.928	0.925
	R	0.971	0.961	0.989	0.963	0.962
Redlich-Peterson	K_{RP} (L/mg)	17.16	1.069	3.314	6.329	1.538
	α_{RP}	3.623	0.301	0.202	1.292	40.32
	R^2	0.812	0.958	0.938	0.985	0.948
	R	0.901	0.978	0.968	0.992	0.973

where K_{RP}, α_{RP} and β are constants in this equation. The constants K_{RP} and α_{RP} are found from the slope and intercept of a linear plot of C_e/q_e *vs.* C_e (Table-6). When several adsorption isotherms are analyzed, it becomes clear that the Schiff base doped PANI composites have a higher sorption capacity than PANICl.

Surface area and polyfunctional groups are typically two parameters that influence maximum adsorption capacity. While polyfunctional groups offer a lot of active sites for the adsorption reaction, substantial surface area ensures that the solid adsorbent has enough contact with metal ions in aqueous solutions.

Effect of temperature: To determine whether the sorption process is physisorption or chemisorption, the impact of temperature on the adsorption process is investigated in the range of 303-318 K. The observed q_e values were found to decrease with increase in temperature for all the composites. Therefore, adsorption of metal ion favours physisorption.

In order to analyze the thermodynamic parameters for the adsorption of mercuric ions on PANI-Schiff base composites the distribution coefficients (K_d) were calculated using eqn. 6:

$$K_d = \frac{q_e}{C_e} \qquad (6)$$

where q_e is the amount of metal adsorbed on the unitary sorbent mass at equilibrium and C_e represents the equilibrium concentration of metal ions in solution.

Thermodynamic parameters: The standard enthalpy change ($\Delta H°$), free energy change ($\Delta G°$) and entropy change ($\Delta S°$) were calculated using van't Hoff equation (eqn. 7):

$$\Delta G° = -RT \ln K_d \qquad (7)$$

where R = universal gas constant (8.314 J mol^{-1} K^{-1}).

$$\ln K_d = \frac{\Delta H°}{RT} + \frac{\Delta S°}{R} \qquad (8)$$

The slope and intercept of the plot of $\ln K_d$ *vs.* $1/T$ are used to determine the values of $\Delta H°$ and $\Delta S°$.

The $\Delta G°$ values that are negative indicate the spontaneity of the adsorption process. A further indication that adsorption is more likely at high temperatures is the decline in $\Delta G°$ values with increasing temperature. The $\Delta G°$ values found in this investigation suggested that the adsorption may involve physisorption. Adsorption is an exothermic process, as indicated by negative values of ($\Delta H°$). Positive values of ($\Delta S°$) indicate greater unpredictability at the solid/solution interface during Hg(II) ion adsorption onto PANI composites (Table-7).

Additionally, the physisorption process, which may also contribute to the overall adsorption process, might result in an increase in entropy due to the release of water molecules from hydrated ions or water molecules that are already present on the surface.

Effect of time: All the polymeric composites under investigation were equilibrated in the HgCl$_2$ solution (0.02 M) for different periods of time (10-60 min) in an ultrasonic bath (Table-8). From the results, it is inferred that the optimum sonication time is 30 min for the maximum adsorption.

TABLE-7
THERMODYNAMIC PARAMETERS FOR THE ADSORPTION OF HgCl$_2$ ON VARIOUS PANI SCHIFF BASE COMPOSITES

Thermodynamic parameters	PT2ClB	PTTE	PTP2ClB	PTPTE
$-\Delta G°$ (kJ mol^{-1})	0.562	4.458	5.07	0.562
	3.083	3.71	4.121	0.951
	2.577	2.858	2.57	1.318
	0.985	2.077	1.692	2.011
$\Delta H°$ (kJ mol^{-1})	-8.313	-6.216	-8.923	-3.277
$\Delta S°$ (J)	25.66	18.72	27.39	11.01
R^2	0.927	0.997	0.985	0.965

TABLE-8
EFFECT OF TIME ON THE ADSORPTION OF HgCl$_2$

Time	PT2ClB	PTTE	PTP2ClB	PTPTE
10	7.5	75.0	73.0	18.5
20	12.5	66.0	67.0	17.5
30	20.0	82.5	79.0	20.0
40	10.0	63.0	60.0	18.0
50	7.5	70.0	67.0	19.0
60	5.0	74.0	72.0	19.5

Effect of pH: Desorption-sorption of Hg^{2+} ions by PANI salts are mostly reversible and the processes can be controlled by changing the pH of the solution. To have better understanding of the adsorption mechanism, the effect of variation of pH on the adsorption process was examined in the pH range of 1-13. HCl was used to monitor the extent of adsorption at low pH while sorption behaviour at high pH was understood using NaOH. The adsorption capacities are found to be less at low pH values and increase with increase in pH (Table-9). At low pH PANI exists as PANI (+) and mercuric chloride is adsorbed on to the active sites through chloride bridge and H-bonding.

TABLE-9
EFFECT OF pH ON THE ADSORPTION OF HgCl$_2$

pH	PT2ClB	PT4ClB	PTTE	PTP2ClB	PTPTE
1	30.0	7.5	30.0	30.0	32.5
2	50.0	22.5	42.5	37.5	30.0
3	40.0	30.0	7.5	12.5	27.5
4	45.0	17.5	40.0	40.0	15.0
5	47.5	40.0	45.0	22.5	25.0
6	25.0	25.0	30.0	30.0	30.0
8	27.5	35.0	27.5	12.5	22.5
9	20.0	22.5	20.0	25.0	25.0
10	32.5	37.5	27.5	32.5	27.5
11	22.5	27.5	25.0	35.0	35.0
12	32.5	20.0	32.5	22.5	22.5
13	42.5	35.0	40.0	25.0	27.5

The competing adsorption of H$^+$ ions and metal ions for the same active adsorption site can account for this. The decrease in proton competition for the adsorption sites causes the adsorption surface to become less positive as the pH increases. As a result, it is anticipated that there will be an increase in the electrostatic attraction and ion-exchange between the metal ions and the surface of the composite. Mercuric chloride is absorbed by the emaraldine base form of PANI-Schiff base compound in the alkaline range of pH 9-13.

Effect of PANI-Schiff base composites: To understand the effect of varying the amount of PANI-Schiff base composites on adsorption process, a constant concentration of 0.02 M $HgCl_2$ was used. The plots of weight of PANI-Schiff base composite *vs.* q_e were curved and thus non-linear. The optimum weight of polymer composites required was found to be 0.002 g for all the composites (Table-10).

TABLE-10
EFFECT OF PANI SCHIFF BASE COMPOSITES
ON THE ADSORPTION OF $HgCl_2$

Weight of PANI composite	PT2ClB	PTTE	PTP2ClB	PTPTE
0.001	25.0	76.0	73.0	20.0
0.002	20.0	67.5	70.0	15.0
0.003	15.0	64.5	66.0	10.0
0.004	10.0	57.5	63.0	7.5
0.005	5.0	50.5	59.0	2.5

Conclusion

Due to its efficacy even at low pollutant concentrations, selectivity and cost effectiveness, the adsorption process is regarded as the most promising method. In summary, novel organic adsorbents, polyaniline doped with Schiff base were used as adsorbents to eliminate mercury ions from the aqueous solutions. Both mono layer and multi-layer adsorptions occur concurrently on the surface of the adsorbents, according to results supported by the Langmuir, Freundlich, Temkin, Dubinin-Radushkevich and Redlich-Peterson models. The viability of the adsorption process is shown by the negative values of the free energy of activation and the positive values of the entropy of activation. For all adsorbents, 30 min has been shown to be the ideal sonication time. Spectral information, a SEM micrograph and PXRD analysis have all supported the mercuric ions adsorption on the PANI matrix.

CONFLICT OF INTEREST

The authors declare that there is no conflict of interests regarding the publication of this article.

REFERENCES

1. M. Abdulkarim and F.A. Abu Al-Rub, *Adsorpt. Sci. Technol.*, **22**, 119 (2004);
    https://doi.org/10.1260/026361704323150908
2. V.K. Gupta, C.K. Jain, I. Ali, M. Sharma and V.K. Saini, *Water Res.*, **37**, 4038 (2003);
    https://doi.org/10.1016/S0043-1354(03)00292-6
3. D. Mohan and K.P. Singh, *Water Res.*, **36**, 2304 (2002);
    https://doi.org/10.1016/S0043-1354(01)00447-X
4. P. Vasudevan, V. Padmavathy and S.C. Dhingra, *Bioresour. Technol.*, **89**, 281 (2003);
    https://doi.org/10.1016/S0960-8524(03)00067-1
5. B.F. Noeline, D.M. Manohar and T.S. Anirudhan, *Sep. Purif. Technol.*, **45**, 131 (2005);
    https://doi.org/10.1016/j.seppur.2005.03.004
6. A. Bentouami and M.S. Ouali, *J. Colloid Interface Sci.*, **293**, 270 (2006);
    https://doi.org/10.1016/j.jcis.2005.06.040
7. N.A.A. Qasem, R.H. Mohammed and D.U. Lawal, *npj Clean Water*, **4**, 36 (2021);
    https://doi.org/10.1038/s41545-021-00127-0
8. J. Mishra, R. Saini and D. Singh, *IOP Conf. Ser.: Mater. Sci. Eng.*, **1168**, 012027 (2021);
    https://doi.org/10.1088/1757-899X/1168/1/012027
9. A. Yadv, P. Choudhary and A. Kumar, *J. Indian Forensic Med.*, **36**, 1 (2014).
10. D.M. Manohar, K.A. Krishnan and T.S. Anirudhan, *Water Res.*, **36**, 1609 (2002);
    https://doi.org/10.1016/S0043-1354(01)00362-1
11. A. Denizli, S. Senel, G. Alsancak, N. Tüzmen and R. Say, *React. Funct. Polym.*, **55**, 121 (2003);
    https://doi.org/10.1016/S1381-5148(02)00221-3
12. R.K. Gupta, R.A. Singh and S.S. Dubey, *Sep. Purif. Technol.*, **38**, 225 (2004);
    https://doi.org/10.1016/j.seppur.2003.11.009
13. R. Ansari and F. Raofie, *E-J. Chem.*, **3**, 35 (2006);
    https://doi.org/10.1155/2006/523275
14. K. Kadirvelu, P. Kanmani, P. Senthilkumar and V. Subburam, *Adsorpt. Sci. Technol.*, **22**, 207 (2004);
    https://doi.org/10.1260/0263617041503480
15. K. Anoop Krishnan and T.S. Anirudhan, *J. Hazard. Mater.*, **92**, 161 (2002);
    https://doi.org/10.1016/S0304-3894(02)00014-6
16. A.M.M. Vargas, A.L. Cazetta, M.H. Kunita, T.L. Silva and V.C. Almeida, *Chem. Eng. J.*, **168**, 722 (2011);
    https://doi.org/10.1016/j.cej.2011.01.067
17. A. Eisazadeh, H. Eisazadeh and K.A. Kassim, *Synth. Met.*, **171**, 56 (2013);
    https://doi.org/10.1016/j.synthmet.2013.03.014
18. M. Hallajiqomi and H. Eisazadeh, *J. Ind. Eng. Chem.*, **55**, 191 (2017);
    https://doi.org/10.1016/j.jiec.2017.06.045
19. D. Mahanta, G. Madras, S. Radhakrishnan and S. Patil, *J. Phys. Chem. B*, **112**, 10153 (2008);
    https://doi.org/10.1021/jp803903x
20. M.S. Mansour, M.E. Ossman and H.A. Farag, *Desalination*, **272**, 301 (2011);
    https://doi.org/10.1016/j.desal.2011.01.037
21. Y. Zhang, Q. Li, L. Sun, R. Tang and J. Zhai, *J. Hazard. Mater.*, **175**, 404 (2010);
    https://doi.org/10.1016/j.jhazmat.2009.10.019
22. I.M. Mustafa, M.A. Hapipah, M.A. Abdulla and T.R. Ward, *Polyhedron*, **28**, 3993 (2009);
    https://doi.org/10.1016/j.poly.2009.10.004
23. S. Radhakrishnan, R. Balakrishnan and A. Selvaraj, *Orient. J. Chem.*, **36**, 780 (2020);
    https://doi.org/10.13005/ojc/360426
24. J.B. Yadav, Advance Practical Physical Chemistry, 14th Edition, Goel Publishing House, New Delhi, India (1995).
25. R.M. Silverstein, G.C. Bassler and T.C. Morril, Spectrometric Identification of Organic Compounds, 5th ed., Wiley: New York, p. 110 (1991).
26. M. Reka Devi, B. Lawrence, N. Prithivikumaran and N. Jeyakumaran, *Int. J. Chemtech Res.*, **6**, 5400 (2014).
27. S.K. Das, A.R. Das and A.K. Guha, *Environ. Sci. Technol.*, **41**, 8281 (2007);
    https://doi.org/10.1021/es070814g
28. J. Wang, B. Deng, H. Chen, X. Wang and J. Zheng, *Environ. Sci. Technol.*, **43**, 5223 (2009);
    https://doi.org/10.1021/es803710k